Computational Modeling of Close-In Millimeter Wave Radar for the Detection of Concealed Threats

Kathryn Williams, Carey M. Rappaport, Ann W. Morgenthaler, Jose Martinez, Richard Obermeier, Fernando Quivira
Contact: williams.ka@neu.edu

Abstract

The full-wave Finite Difference Frequency Domain (FDFD) algorithm is being used to model millimeter-wave scattering responses from the human body illuminated by various source configurations, including a small aperture, close-in detector and a focusing transmitting reflector. In both cases the sensing probe is used to determine the presence of a foreign object underneath clothing. Modeling is used to determine the feasibility of feature detection at this range and to investigate optimal antenna designs. Forward modeling with FDFD allows the scattered field over the entire computational domain to be viewed, which provides insight into ideal antenna placement. 2D FDFD also generates accurate synthetic data for computational experiments and provides a basis for model-based inversion.

Relevance

The current state-of-the-art portal-based scanning technology uses a monostatic radar configuration and a 2D maximum intensity projection to display the resulting images (simulated in Figs 1 and 2 shown for front-view and rotated 60˚). These images lack detail at all angles except the specular angle, resulting in a flat, two dimensional picture with little curvature. This provides motivation for investigating alternative antenna positions that could result in improved imaging of anomalous objects on the body.

Fig 1. 2D rendering, front view

Fig 2. 2D rendering, rotated 60˚

Figs 3 and 4 show a three-dimensional rendering of the body, created by adjusting the lighting features in medical visualization software for the data sets of Figs 1 and 2. Figs 3 and 4 reveal more information about the curvature and other features on the body. This concept applies to current systems, where certain sensor configurations, such as multistatic systems, are able to reveal more information about the subject. Although current systems calculate depth information, they do not display it in an easily-viewable form.

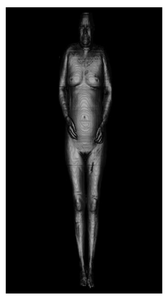

Fig 3. 3D rendering, front view

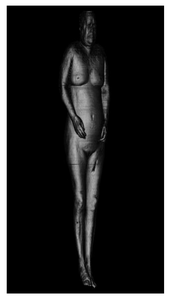

Fig 4. 3D rendering, rotated 60 ˚

Modeling

Cryosection slice images of a human torso were taken from the Visible Human Project and used for accurate full-wave 2D FDFD modeling. One slice used is shown in Fig 5.

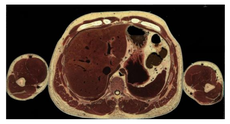

Fig 5. Human slice used for modeling geometry

A small aperture close-in 20GHz confirmation detector was investigated using FDFD to identify scattering features. A simple monostatic sensor of this type might be used for local detection of foreign objects under clothing by detecting changes in the received signal relative to the received signal when no object is present. A point source illumination with a bandwidth of 1.5GHz is used as the incident field. The point source was repositioned around the body, at distances of 2'' and 4'' and approximately following the contour of the body. Foreign objects were introduced into the model to simulate anomalous objects and unusual contours. These objects included a block of metal (2cm thick), a block of TNT (2cm thick), and a metal pipe (3/4'' in diameter). The scattered field from these geometries were compared with the scattered fields from a body with no foreign objects present. Figs 6-8 illustrate the point source at various locations for no object, a flat metal object, and a metal pipe. These figures show the geometry of the body (in black), the position of the point source (white circle) and the magnitude of the scattered field.

Fig 6a. Scattered field from Body, Source Position 1

Fig 6b. Scattered field from Body, Source Position 2

Fig 6c. Scattered field from Body, Source Position 3

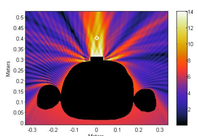

Fig 7a. Scattered field from Metal, Source Position 1

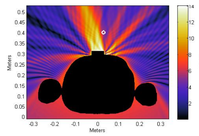

Fig 7b. Scattered field from Metal, Source Position 2

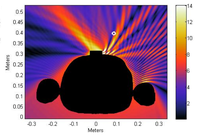

Fig 7c. Scattered field from Metal, Source Position 3

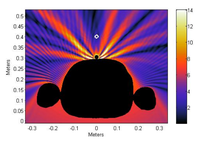

Fig 8a. Scattered field from Metal Pipe, Source Position 1

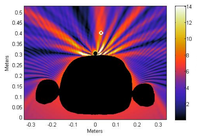

Fig 8b. Scattered field from Metal Pipe, Source Position 2

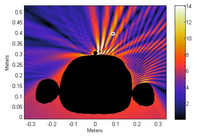

Fig 8c. Scattered field from Metal Pipe, Source Position 3

The magnitude of the returned signal at the source varies with source position and with material and material shape. This effect is notable in Figs 6a, 7a, and 8a, where the source is positioned directly above the foreign object and material shape varies. A more sophisticated multistatic configuration would record and reveal the strong scattered waves in other directions and enable better detection of anomalous objects. Figs 9 and 10 show the time domain response at an array of receivers for a body with no objects present and for a body with a metal object. The metal is a rough perturbation to the smooth skin surface, which interrupts the continuous scattered pulse that would otherwise leave the body. This is shown by the null at position 60 in Fig 10.

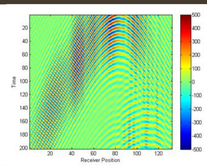

Fig 9a. Time domain scattered signal for an array of receivers and one transmitter position (body with no target)

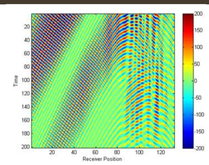

Fig 9b. Time domain scattered signal for an array of receivers and a different transmitter position (body with no target)

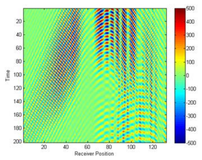

Fig 10a. Time domain scattered signal for an array of receivers and one transmitter position (body with metal)

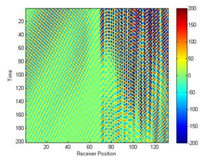

Fig 10b. Time domain scattered signal for an array of receivers and a different transmitter position (body with metal)

Extending 2D FDFD to 2½D FDFD

Although 2D models were used in the simulations presented here, 2½D is being investigated as a more accurate method of modeling scattering from the human body. 2½D algorithms are more flexible than 2D, but are not as computationally intensive as 3D methods. Unlike 2D, 2½D methods can model geometries that vary in one direction and can implement sources that have propagation in that direction. Fig 11 shows one type of geometry that can be modeled with 2½D FDFD, where the geometry varies slowly in the z direction.

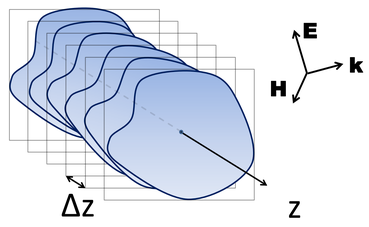

Fig 11. 2 ½D geometry

The 2½D FDFD simulation requires two wave equations to be solved simultaneously for both longitudinal field components E_z and H_z, rather than solving a single wave equation for E_z (TM) or H_z (TE) as is done in the 2D FDFD algorithm.

- All field components given by: $F_n(x,y,z) = F_{n0}(x,y,az)\, e^{ik_z z}$ where a is small
- Materials (ϵ & μ) slowly vary in z. If they are independent of z, then $a = 0$.
- k_z is not necessarily small
- Generalized "TM" wave equation (generalized "TE" equation is dual):

$$\frac{\partial}{\partial x}\left[\left(\frac{k}{k_T}\right)^2\frac{1}{\mu}\frac{\partial E_{z0}}{\partial x}+\frac{2\omega k k_z}{k_T^4}\frac{\partial k}{\partial y}H_{z0}+\left(\frac{k}{k_T}\right)^2\frac{J_{my0}}{\mu}-a\left(\frac{k}{k_T}\right)^2\frac{1}{\mu}\frac{\partial E_{x0}}{\partial z}\right]+$$
$$\frac{\partial}{\partial y}\left[\left(\frac{k}{k_T}\right)^2\frac{1}{\mu}\frac{\partial E_{z0}}{\partial y}-\frac{2\omega k k_z}{k_T^4}\frac{\partial k}{\partial x}H_{z0}-\left(\frac{k}{k_T}\right)^2\frac{J_{mx0}}{\mu}-a\left(\frac{k}{k_T}\right)^2\frac{1}{\mu}\frac{\partial E_{y0}}{\partial z}\right]+$$
$$\frac{k^2}{\mu}E_{z0}+a\frac{i\omega^2 k_z}{k_T^2}\left(\frac{\partial \epsilon}{\partial z}E_{z0}+\epsilon\frac{\partial E_{z0}}{\partial z}\right)=-\frac{i\omega k^2 J_{z0}}{k_T^2}+\frac{i\omega^2 k_z \rho_0}{k_T^2}-$$
$$\frac{2\omega k_z k}{k_T^4}\left(J_{x0}\frac{\partial k}{\partial x}+J_{y0}\frac{\partial k}{\partial y}\right)+a\frac{2\omega k_z k}{k_T^4}\left(\frac{\partial k}{\partial y}\frac{\partial H_{x0}}{\partial z}+\frac{\partial k}{\partial x}\frac{\partial H_{y0}}{\partial z}\right)$$

Always part of the equation | Only present if $k_z \neq 0$ | Only present if $a \neq 0$ | Only present if transverse current sources exist | Only present if $a \neq 0$ and $k_z \neq 0$

Antenna Design

Forward models give insight into new sensor configuration designs. Fig 12 shows the beam from an elliptical parabola reflector. The beam focuses to illuminate a 1cm thick slice of the body at the second ellipse focal point at 0.6. A circular array of antennas is a possible configuration for receiving the signal.

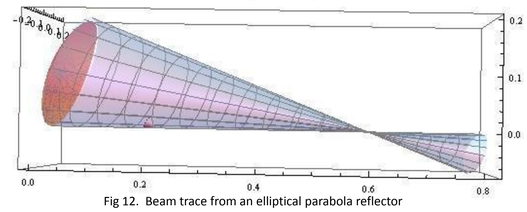

Fig 12. Beam trace from an elliptical parabola reflector

Fig 13 shows the vertical E-field generated by the elliptical reflector as modeled by FDFD, corresponding to Fig 12. The focused beam gives a high-intensity spot at 0.6. A close-up of the power density at this spot indicates a high-intensity 1cm tall, 12cm long "blade", propagating in the direction of the blade (as indicated by the arrows in Fig 14).

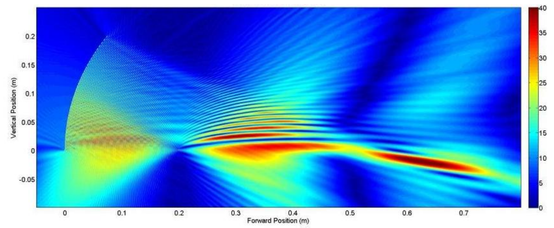

Fig 13. Vertical E-field component from the reflector

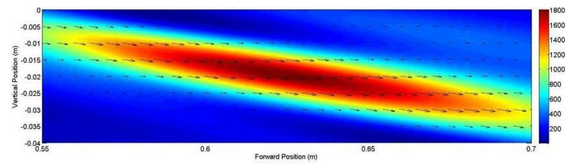

Fig 14. Poynting Vector of Beam

Accomplishments Through Current Year

Computational modeling of a small-aperture, close in millimeter wave radar was performed this year. 2½D algorithms were developed as part of a suite of computational tools being created at Northeastern University.

Future Work

Future work includes modeling with the 2½D methods, continuing to investigate optimal antenna positions and multistatic system configurations, and validating and inverting measured data from a novel prototype radar setup.

References

[1] Morgenthaler, A., *Coupled Wave Equations for 2 ½ D FDFD Simulations,* 2010.
[2] Fernandes, J., *Millimeter-Wave Imaging of Person-Borne Improvised Explosive Devices,* MS Thesis, Dept. Elect. Eng., Northeastern Univ., Boston, MA 2010
[3] Morgenthaler, A., and Rappaport, C., (2010). *Extending 2D FDFD Modeling to 2 ½ Dimensions for Realistic Simulation of Millimeter Wave Radar Whole-Body Imaging*

This material is based upon work supported by the U.S. Department of Homeland Security under Award Number 2008-ST-061-ED0001. The views and conclusions contained in this document are those of the authors and should not be interpreted as necessarily representing the official policies, either expressed or implied of the U.S. Department of Homeland Security.